# Synergistic Use of Bithiazole and Pyridinyl Substitution for Effective Electron Transport Polymer Materials

Carolyn Buckley<sup>†</sup>, Simil Thomas<sup>†</sup>, Michael McBride<sup>‡</sup>, Zhibo Yuan<sup>†</sup>\*\*, Guoyan Zhang<sup>‡</sup>, Jean-Luc Bredas<sup>†</sup>, and Elsa Reichmanis<sup>†</sup>\*

†School of Chemistry and Biochemistry, Georgia Institute of Technology, 901 Atlantic Dr NW, Atlanta, GA 30332-0400

\*School of Chemical and Biomolecular Engineering, Georgia Institute of Technology, 311 Ferst Dr NW, Atlanta, GA, 30332-0400

§School of Materials Science and Engineering, Georgia Institute of Technology, 771 Ferst Drive NW, Atlanta, GA 30332

ABSTRACT: The development of semiconducting conjugated polymers for organic field effect transistors (OFETs) has been the focus of intense research efforts for their key role in plastic electronics, as well as a vision of solution processability leading to reduced costs in device fabrication relative to their inorganic counterparts. The pursuit of high-performance n-channel (electron transporting) polymer semiconductors vital to the development of robust and low-cost organic integrated circuits has faced significant challenges; mainly for poor ambient operational stability and OFET device performance lagging far behind that of pchannel organic semiconductors (OSCs). As an alternative to the ubiquitous donor-acceptor (DA) molecular design strategy, an all-acceptor (AA) unipolar approach was implemented in the design of poly(2-(2-decyltetradecyl)-6-(5-(5'-methyl-[2,2'-bithiaol]-5-yl)-3-(5-methylpyridin-2-yl)-5-(tricosan-11yl)-2,5-dihydropyrrolo[3,4-c]pyrrole-1,4-dione) (**PDBPyBTz**). The *n*-channel copolymer allowed investigation of the impact of electron withdrawing moieties on conjugated polymer device performance and the utility of the AA molecular design strategy. As an analog to benzene, the pyridines flanking the diketopyrrolopyrrole moiety in PDBPyBTz were strategically chosen to lower the energy levels and impart planarity to the monomer, both of which aid in achieving stable n-channel performance. Incorporation of PDBPyBTz into a bottom-gate-bottom-contact OFET, afforded a device that exhibited unipolar electron transport. In addition to developing a high-performance n-channel polymer, this study allowed for an investigation of structure-property relationships crucial to the design of such materials in high demand for sustainable technologies including organic photovoltaics and other solution-processed organic electronic devices.

#### 1. Introduction

The development of polymeric semiconductors for use in organic field effect transistors (OFETs) has been the subject of intense research focus for its potential in realizing low-cost, large-area, and flexible devices such as sensors, displays, radio frequency identification tags, etc.<sup>1-4</sup> While significant progress

has been made in high-performance p-channel materials, that of their n-channel counterparts lags far behind.<sup>5-8</sup> In order to enable the implementation of complementary organic-semiconductor (complementary metal-oxide semiconductor-like) logic circuits, it is imperative to improve the electron mobility and ambient stability of unipolar n-channel conjugated polymers, while maintaining processability.<sup>9</sup> The prevailing donor-acceptor (D-A) design motif has led to significant advances in polymer semiconductor performance as it allows for the fine-tuning of frontier molecular orbitals for efficient charge injection in addition to promoting strong intermolecular  $\pi$ - $\pi$  stacking interactions that facilitate charge transport.<sup>8,10</sup> This design strategy, however, has proven to be of limited use in developing n-channel conjugated polymers because there are relatively few building blocks with sufficient electron deficiency to achieve an electron affinity higher than +4 eV (*i.e.*, roughly speaking, a lowest unoccupied molecular orbital (LUMO) energy below -4 eV) for facile electron injection and operational stability of resultant polymers. In addition, the decrease in ionization potential and electron affinity (destabilization of the highest-occupied molecular orbital (HOMO) and LUMO energy levels) upon incorporation of a donor unit often leads to ambipolar behavior in OFET devices, which can lead to unbalanced hole/electron mobilities, undesirable leakage currents and small current on/off ratios ( $I_{ON}/I_{OFF}$ ).<sup>11-17</sup>

The use of all-acceptor (A-A) polymers to minimize intramolecular charge transfer and preserve polymer low lying frontier molecular orbitals (FMOs) has been demonstrated to successfully result in unipolar n-channel materials upon incorporation into conventional transistor devices. <sup>18–24</sup> Performance improvements were observed because the increased electron affinity facilitated electron injection and the increased ionization potentials diminished hole accumulation. While the synthesis of many acceptor units poses difficulties, the pursuit of high-performance A-A polymers is challenged further by the relative steric bulk of cyano or carbonyl functionalities (in comparison to simple substitutions) common to these electron-deficient moieties. For instance, steric effects can lead to twisted polymer backbones, which negatively impacts molecular packing in thin films and adversely affects charge transport. <sup>15,16,25</sup> While the introduction of a "spacer" unit such as 2,2'-bithiophene (BT) has produced high performance n-channel

polymer semiconductors, <sup>26–28</sup> the electron-rich nature of the thiophene units can also reduce the ionization potential (destabilize the HOMO) and lead to ambipolar behavior. <sup>20</sup>

Sun. et. al. introduced a high-performance ambipolar material based on a pyridine-flanked diketopyrrolopyrrole (DBPy) unit as an acceptor and BT as a donor, which exhibited electron and holemobilities of 6.3 cm<sup>2</sup>V<sup>-1</sup>s<sup>-1</sup> and 2.78 cm<sup>2</sup>V<sup>-1</sup>s<sup>-1</sup>, respectively.<sup>27</sup> Similarly, ambipolar behavior was observed in a copolymer of DBPy and electron-donating thieno[3,2-b]thiophene with a reported mobility of 3.36 cm<sup>2</sup>V<sup>-1</sup>s<sup>-1</sup> for holes and 2.65 cm<sup>2</sup>V<sup>-1</sup>s<sup>-1</sup> for electrons.<sup>29</sup> Unipolar n-channel behavior was observed when hole-injection was suppressed with polyethyleimine (PEI)-modified Au electrodes.<sup>29</sup> Interestingly, Mueller et. al. reported more pronounced n-channel behavior in pyridine-flanked DPP polymers upon fluorination of a thiophene comonomer.<sup>30</sup> Six-membered rings flanking the DPP, diketopyrrolopyrrole, are generally more electron-deficient than five-membered ring alternatives as the six  $\pi$ -electrons are delocalized over a larger ring. The DBPy unit is especially attractive for use in n-channel polymers since the pyridine electronegative nitrogen atom not only serves to lower the FMOs vs. phenyl rings, but also relieves steric interactions between the lactam oxygen atoms and the α-hydrogen atoms present in diphenyl-DPPs.<sup>31</sup> Our quantum-chemical calculations corroborate the previously reported 0° dihedral angle seen between the pyridine and the DPP core (vide infra), making the DBPy unit completely planar.<sup>27</sup> The high electron mobilities seen in DBPy – based ambipolar polymeric semiconductors suggest that the pyridine substituted moiety may be a promising acceptor for incorporation into A-A copolymers.

A viable second acceptor unit, namely 2,2'-bithiazole (BTz), might be considered as an effective comonomer. In contrast to the more commonly used BT, BTz is more electron-deficient due to the presence of an electronegative nitrogen atom within the five-membered ring that serves to increase the electron affinity.<sup>32</sup> The interaction between the nitrogen lone pairs and antibonding orbitals in the adjacent thiazole rings facilitate 'locking' the BTz unit into a planar conformation,<sup>32</sup> in contrast to the BT analog that exhibits a dihedral angle of ~30°.<sup>33</sup> Recently, we developed a synthetic strategy for the facile incorporation of BTz into conjugated polymers, and further demonstrated that the replacement of BT with

BTz increases the electron affinity of the resultant polymer thereby promoting n-channel charge transfer characteristics as determined by OFET performance.<sup>34</sup> The BTz and thiophene-flanked DPP D-A copolymer exhibited an electron mobility of 0.3 cm<sup>2</sup>V<sup>-1</sup>s<sup>-1</sup> in top-contact/bottom gate (TCBG) OFET devices.<sup>34</sup> Subsequently, BTz was polymerized with DPP to afford a dithiazole-DPP A-A copolymer having a unipolar field-effect mobility up to 0.067 cm<sup>2</sup>V<sup>-1</sup>s<sup>-1</sup> in a bottom-gate/bottom-contact (BGBC) device.<sup>18</sup>

Herein, we report the copolymerization of the BTz distannane monomer with a brominated DBPy to afford an all-acceptor, unipolar n-channel polymer, poly(dipyridinyldiketopyrrolopyrrole-bithiazole), PDBPyBTz, as shown in Scheme 1. With the combination of two planar electron-deficient units, both of which had demonstrated high electron mobility in isoelectronic conjugated polymer precursors, poly(dithienyldiketopyrrolopyrrole-bithiazole) PDBTz and poly(dipyridinyldiketopyrrolopyrrole-bithiophene) PDBPyBT, we explore and contrast the optoelectronic properties and device performance characteristics of this new 'all acceptor' polymer semiconducting material with these analogous structures. The computational, photophysical, morphological and device investigations demonstrate that the all-acceptor approach with judicious choice of molecular structural moieties can lead to the design and development of effective electron transport semiconducting materials.

#### 2. Results

# 2.1 Polymer Synthesis and Thermal Properties

The synthesis of **PDBPyBTz** is outlined in Scheme 1, and complete synthetic details are provided in the supporting information, with NMR spectra given in Figures S1 and S2.

Scheme 1. Synthetic route to prepare PDBPyBTz

The 11-(bromomethyl)tricosane side chain (1) was synthesized according to literature procedures in 72% yield. The synthesis of 3,6-bis(5-bromopyridin-2-yl)-2,5-dihydropyrrolo[3,4-c]pyrrole-1,4-dione (2) was completed in 30.9 % yield by reacting commercially available 5-bromopyridine-2-carbonitrile with diethyl succinate in the presence of potassium t-butoxide in 2-methyl-2-butanol. Subsequent alkylation at the N – positions on the DPP core with 2-decyl-1-tetradecylbromide gave 3,6-bis(5-bromopyridin-2-yl)-2,5-bis(2-decyltetradecyl)-2,5-dihydropyrrolo[3,4-c]pyrrole-1,4-dione (3) in 59% yield. Homocoupling of commercially available 2-bromothiazole yielded 2,2'-bithiazole (4) in 80% yield, which was then stannylated to afford 5 in 69% yield. Stille coupling of 4 with freshly prepared 5 under

microwave irradiation (100 °C for 1 hour) produced the target polymer **PDBPyBTz**, which was purified via Soxhlet extraction (see SI for synthetic details). The weight ( $M_W$ ) and number ( $M_N$ ) average molecular weights of **PDBPyBTz** were 11,850 and 6,900 g/mol, respectively, with a dispersity (D) of 1.71, determined using high-temperature gel-permeation chromatography (HT-GPC) at a column temperature of 135 °C with 1,3,5-trichlorobenzene as eluent (see Figure S3 in Supporting Information). **PDBPyBTz** is stable up to 335 °C (see TGA characterization, Figure S4a in SI). DSC characterization (Figure S4b, SI) showed a glass transition temperature at 67 °C but no other thermal transitions up to 290°C.

**PDBTz** was synthesized according to literature procedures<sup>34</sup> using **1** as the side chain, with a  $M_W$  of 46,175,  $M_N$  of 12,042 g/mol and D of 3.83 (Figure S5). A commercial sample of **PDBPyBT** was purchased from Ossila chemical, and found to have a  $M_W$  of 29,300,  $M_N$  of 11,350, and D of 2.58 (Figure S6). GPC analysis was performed under the same conditions for all polymers for consistency.

# 2.4 Computational Methodology

The geometry optimizations of the **PDBPyBTz** oligomers were performed with the ωB97XD functional and 6-31G(d,p) basis set using the Gaussian 09 Revision D.01 suite of programs.<sup>37</sup> To explore the torsion potential landscape of the polymer building blocks, the total energies as a function of the dihedral angles between the pyridine-thiazole and pyridine-DPP units were calculated at the same level of theory, by fixing the dihedral angles and relaxing all other geometrical degrees of freedom (Figure S7, SI). We note that the side-alkyl chains in the **PDBPyBTz** units were replaced with methyl groups to save computational time.

The electronic and optical properties of the  $\pi$ -conjugated polymer were calculated as well at the tuned- $\omega$ B97XD-6-31G(d,p) level of theory. The range separation parameter  $\omega$  was optimized following the IP tuning procedure<sup>38,39</sup> and within the self-consistent reaction field (SCRF) framework (taking into account a dielectric constant  $\varepsilon = 4.7$ , equivalent to chloroform, to maintain consistency with

experiment); the tuned  $\omega$  value is 0.003 Bohr<sup>-1</sup> in the case of the tetramer. The optical properties were evaluated using time-dependent density functional theory (TDDFT) with the same functional and basis set.

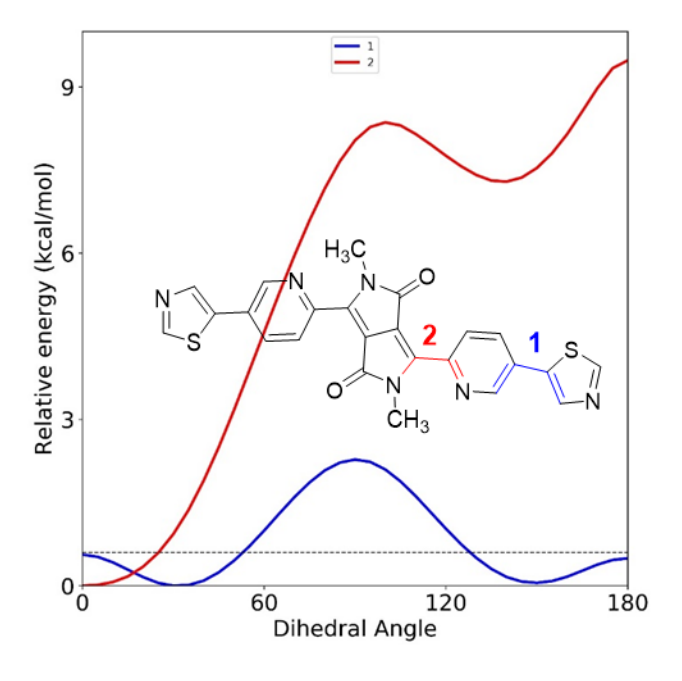


**Figure 1.** Illustration of the torsion potentials between the pyridine and thiazole units (1) and the pyridine and DPP units (2) for the PDBPyBTz monomer, as calculated at the tuned- $\omega$ B97X-D/6-31G(d,p) level of theory ( $\omega$ =0.14 Bohr<sup>-1</sup>). The dotted line represents thermal energy at 300 K (=0.6 kcal mol<sup>-1</sup>).

The torsion potential between the pyridine and thiazole units has minima around 30° and 150° (**Figure 1**). The barrier height separating these two minima in the case of the isolated monomer is small, ca. 2.4 kcal mol<sup>-1</sup> (that is, about 4 times the thermal energy kT at room temperature, 0.6 kcal mol<sup>-1</sup>); hence, the transition from a *syn* conformation (with the pyridine nitrogen on the same side as the thiazole nitrogen) to an *anti*-conformation is possible. Also, the flatness of the torsional potentials around the minima means that there can be fluctuations of  $\pm 30^{\circ}$  around each of the minima in the case of an isolated chain and that inter-chain interactions in the solid state could lead to (nearly) coplanar conformations. We note that a similar torsion angle of ca. 30° was calculated between the DBPy and BT units in the case of the analogous **PDBPyBT** polymer.<sup>27</sup> The evaluation of the torsion potential between the **PDBPyBTz** DPP and pyridine units, see **Figure 1**, also points to a strongly preferred coplanar conformation.<sup>34</sup>

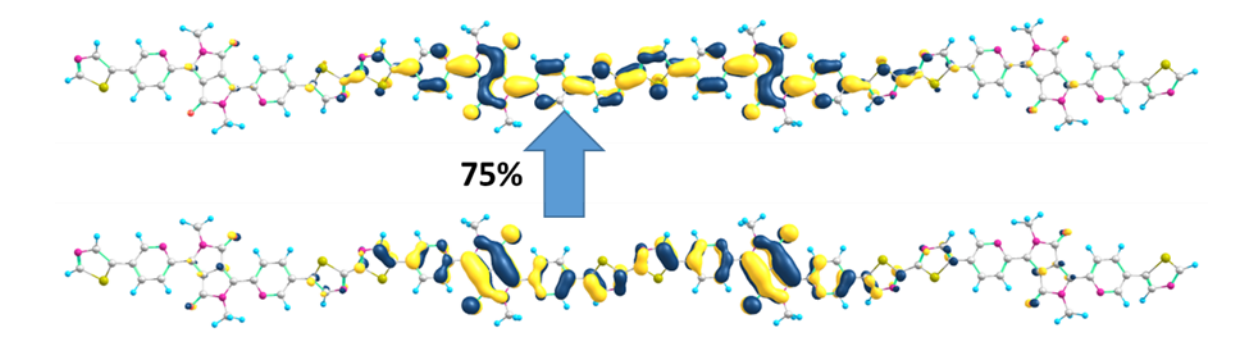


**Figure 2.** Illustration of the major (TD-DFT tuned- $\omega$ B97X-D/6-31G(d,p)) natural transition orbitals (bottom: hole NTO; top: electron NTO) for the S<sub>0</sub> to S<sub>1</sub> vertical transition in the PDBPyBTz) tetramer, evaluated at the S<sub>0</sub> geometry. The weight of the main hole-electron contribution to the excitation is also included.

Calculations of the electronic properties of the **PDBPyBTz** oligomers essentially converge at the level of the tetramer (see Figure S8) and the corresponding optical gap for the polymer chain is 2.07 eV. Figure 2 depicts the DFT-calculated tuned- $\omega$ B97XD natural transition orbitals with the largest contribution to the S<sub>0</sub>-S<sub>1</sub> transition in the **PDBPyBTz** tetramer; it is found that vertical excitation occurs over approximately two repeat units (the second-largest contribution to the S<sub>0</sub>-S<sub>1</sub> transition is shown in Figure S9). There is also another  $\pi$ - $\pi$ \* transition with a significant oscillator strength, which is calculated to appear at 2.9 eV in agreement with the experimental absorption spectra; the NTO analysis shows that in this excitation, the hole is localized on a bithiazole unit while the electron is more delocalized over the polymer chain (overall, this transition has a coupled oscillator nature) (Figure S10).

The highest occupied molecular orbital (HOMO) of the **PDBPyBTz** tetramer is localized on DPP units while the lowest unoccupied molecular orbital (LUMO) is slightly more delocalized across the conjugated backbone (see Figure S11). These characteristics are qualitatively consistent with the calculated band widths (0.12 eV for the upper valence band and 0.22 eV for the lower conduction band) obtained from periodic DFT calculations on a **PDBPyBTz** polymer chain; see the band structure in Figure S12. The calculated effective mass for an electron ( $m^*$ ) is small, 0.23  $m_0$ ; such a small value can give rise to a significant electron mobility provided a band regime can be achieved in the solid state due to the significant inter-chain interactions discussed below in the context of the optical absorption spectra. We

note that, in the case of an isolated chain, an excess electron is calculated to localize nearly over a single DBPy unit with a relaxation energy of *ca.* 0.18 eV (Figure S13).

# 2.2 Photophysical Properties

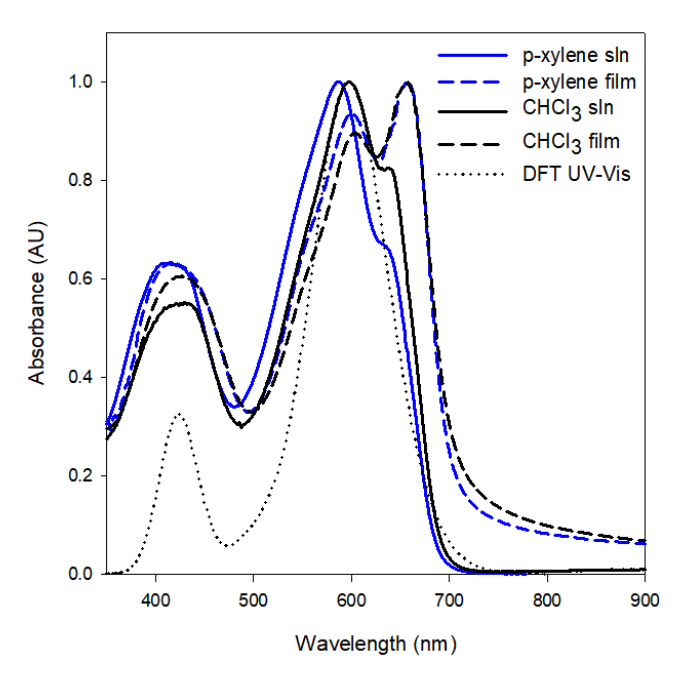


Figure 3. UV-Vis spectra of PDBPyBTz in both solution (1 x  $10^{-6}$  M, chloroform, p-xylene) and thin film, and the calculated TD-DFT spectrum (assuming a surrounding medium with a dielectric constant corresponding to chloroform). Film UV-Vis spectra were obtained by spincoating solutions onto UV-ozone cleaned SiO<sub>2</sub> slides before deposition.

**Table 1**. UV-vis spectral absorption characteristics of **PDBPyBTz** and analogous previously reported polymer structures.

		0-0		0-1		Eg <sup>opt</sup>	
Polymer	Solvent	λ <sub>max</sub> <sup>abs, sln</sup> [nm]	λ <sub>max</sub> <sup>abs, film</sup> [nm]	λ <sub>max</sub> <sup>abs, sln</sup> [nm]	λ <sub>max</sub> <sup>abs, film</sup> [nm]	[eV]	Ref,
PDBPyBTz	CHCl <sub>3</sub>	632	656	591	600	1.47	-
	P-xylene	636	656	588	602	1.47	-
PDPP4Tz	CHCl <sub>3</sub>	715	715	~650	~650	1.34	18
PDPP4T	CHCl <sub>3</sub>	784	786	~710	~710	1.20	28
PDBTz	CHCl <sub>3</sub>	767	765	702	697	1.33	34
PDBPyBt	CHCI <sub>3</sub>	683	695	~630	~650	1.65	27

The UV-vis absorption spectra for both solution and blade-coated thin films of **PDBPyBTz** are presented in **Figure 3**, while the spectral characteristics are summarized in **Table 1**. The more intense absorption bands between 550-700 nm, and the lower intensity bands between 350-450 nm are attributed to  $\pi$ - $\pi$ \* transitions (Figure S10). Minimal positive solvatochromism was seen in the 0-1 blue-shift of  $\lambda_{max}$  from the chloroform to p-xylene solutions, indicating a slight destabilization of this excited state upon decreasing solvent polarity. The  $\lambda_{max}$  of the chloroform solution (632 nm) and thin film (656 nm) for the 0-0 transition of **PDBPyBTz** is blue-shifted from that of its bithiophene analog, **PDBPyBT** (683 nm and 695 nm, respectively). This is consistent with the lesser electron-rich nature of **PDBPyBTz** that consists of two acceptor units, in comparison to that in typical D-A copolymers.

The changes observed in the solution vs. solid-state absorption spectra are consequences of an increase in intermolecular interactions and molecular ordering among the **PDBPyBTz** chains, and can provide insight into the types of aggregates formed, provided that the strengths of the intermolecular excitonic coupling and vibronic coupling are similar.<sup>41</sup> The absorption spectra of the thin films, having similar maxima at 656 nm, are bathochromically shifted from the solution spectra of the polymer in either solvent, which is indicative of J-aggregation according to Kasha's theory.<sup>42</sup> In addition, the ratio of the first two vibronic peak intensities for the 0-0/0-1 transitions is below unity in both solution spectra and becomes inverted in the thin-film absorption spectra. This observation is further evidence of J-aggregation, as it has been shown that with increasing exciton bandwidth, J-[H]-aggregates will show an increase [decrease] in the ratio of the oscillator strengths of the first two vibronic peaks in absorption spectra. <sup>41,43,44</sup> Interestingly, we saw no change in the  $\lambda_{max}$  of the films after annealing above the  $T_g$  at 100 °C for 1.5 hours (see SI). The optical gap ( $E_g^{\text{opt}}$ ) of **PDBPyBTz** evaluated from the solid-state absorption onset is ca. 1.47 eV, which is smaller than that of **PDBPyBTz** evaluated from the solid-state absorption onset is ca.

Photoluminescence spectra of **PDBPyBTz** were obtained for both solution and thin-film, using an excitation wavelength of 637 nm from a continuous-wave laser (Figure S14). The fluorescence spectrum of the thin film had a  $\lambda_{max}$  of 698 nm, while  $\lambda_{max}$  in the solution state was at 679 nm. It should be noted that the fluorescence spectra are not mirror images of the absorption spectra, both being single-peaked and displaying Stokes shifts of 47 and 42 nm for solution and film absorption maxima, respectively.

#### 2.3 Characterization of Electronic Structure

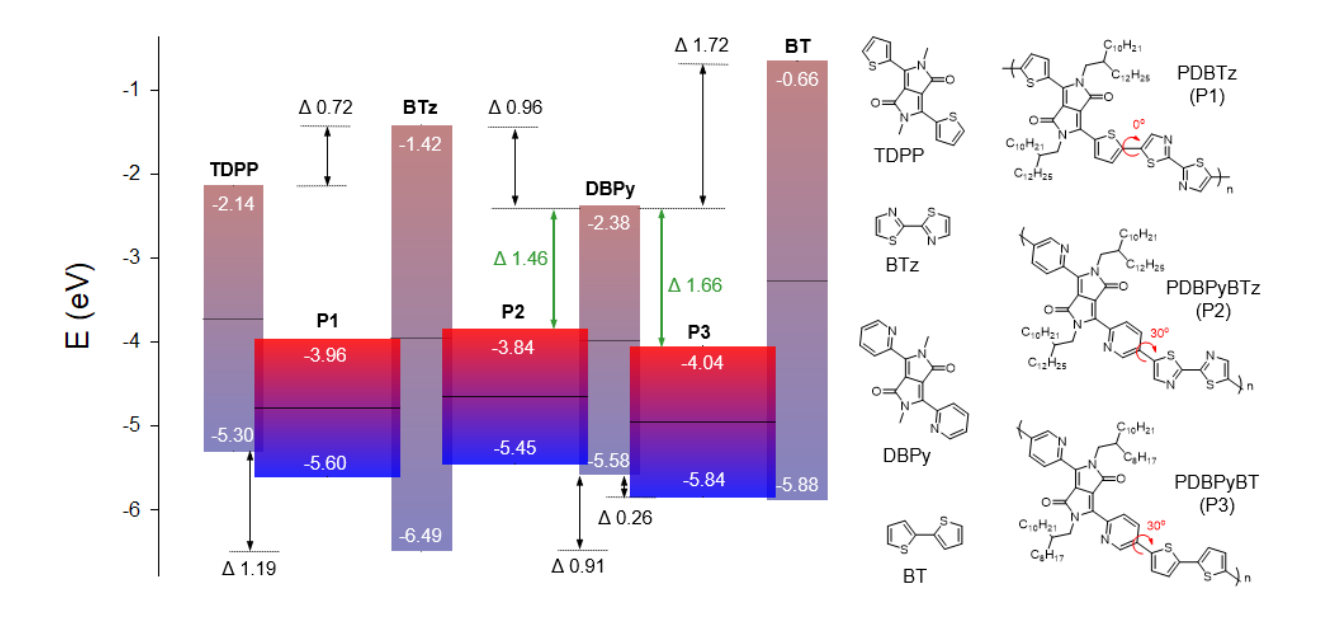


**Figure 4.** Comparison of the DFT-ωB97XD calculated ionization potentials and electron affinities for the monomer units with values for the resultant polymers as estimated from CV, in units of eV. Energy differences between monomer units are given in black, and energy differences between EA energies are given in green.

The redox potentials of **PDBPyBTz**, **PDBTz**, and **PDBPyBT** thin films were investigated using cyclic voltammetry (CV, see Figures S15-S17 in the SI). **PDBPyBTz** exhibits an onset reduction peak at -1.256 V (vs. Fc+/Fc), followed by two reversible reduction peaks at -1.460 V and -1.618 V (vs. Fc/Fc+). The reversibility of the two reductions demonstrates the stability of **PDBPyBTz** as an electron carrier. An onset oxidation potential is seen at 0.346 V (vs. Fc+/Fc), followed by an irreversible oxidation peak at 1.131 V (vs. Fc+/Fc). As the energy of the standard calomel electrode (SCE) is taken to be 4.7 eV vs. vacuum<sup>45</sup>, and Fc+/Fc is +0.380 V vs. SCE<sup>46</sup>, the formal potential of the Fc+/Fc redox couple can be approximated as -5.1 eV on the energy scale.<sup>21,47</sup> With this approximation, the onset oxidation and

reduction potentials correspond to an ionization potential (IP) and electron affinity (EA) of 5.45 and 3.84 eV, respectively, and a transport gap of 1.61 eV. The ionization potentials for **PDBTz** and **PDBPyBT** were estimated in a similar manner, and the results can be seen in Figure 4.

Ultraviolet photoelectron spectroscopy (UPS) was used to determine the intrinsic IP of thin films of **PDBPyBTz**, which was found to be 5.2 eV (Figure S18 in the Supporting Information). With an optical gap of 1.47 eV and an exciton binding energy of approximately 0.14 eV (estimated using the transport gap of 1.61 eV), this would predict an electron affinity of 3.59 eV. Considering the assumptions and uncertainties inherent to conversion factors relating redox potentials to solid-state ionization potentials, we consider the values obtained from the UPS measurements to be consistent with that estimated from the cyclic voltammetry results. <sup>47,48</sup> Both the CV and UPS results of **PDBPyBTz** are suggestive of good ambient stability towards oxidation. <sup>49</sup>

A comparison of the calculated and experimental IPs and EAs between PDBPyBTz, analogous materials PDBTz and PDBPyBT, and component monomers reveals the difficulties in determining structure-property relationships in narrow bandgap polymeric semiconductors (Figure 4). In contrast with previous studies<sup>34,50</sup> and the conventional approach to the D-A (and A-A) design strategy, the substitution of the bithiophene moiety with bithiazole in PDBPyBTz did not result in larger estimated IP and EA values than those observed for PDBPyBT. Similarly, the use of the DBPy moiety did not result in the expected lower ionization energies in comparison to the TDPP moiety.<sup>27</sup> Electrochemical methods of estimating gas-phase ionization potentials present a number of sources of uncertainty which make it difficult to evaluate the precision of these estimations and consequently the qualitative value in comparing estimations between polymer semiconductors.<sup>47,51-53</sup> Indeed, there are minor discrepancies observed between previously reported estimations of IP and EA for PDBPyBT<sup>27</sup>, PDBTz<sup>34</sup>, and those reported here. Bearing these uncertainties in mind, the results can be understood by examining the theoretical MO calculations of the frontier orbital geometries in assessing the effectiveness of π-delocalization in the system. As discussed above, the HOMO coefficients are localized on the DPP aromatic core and

minimally present on the flanking pyridinyl moieties or BTz units (Figure S11). Upon closer inspection, nodes in the HOMO wavefunction can be seen on both the pyridinyl carbon atoms connected to the DPP core and between the atoms connecting the pyridinyl and BTz moieties. Nodes between these units are absent in the LUMO wavefunction, which has greater delocalization along the polymer chain. Similar nodal patterns are seen between the SOMOs of the ions, with the anion wavefunction delocalized across the repeating unit and the cation wavefunction localized on the DPP core (Figure S13). The electronic structure of these wavefunctions may explain why greater LUMO stabilization was seen in **PDBPyBT** than in **PDBPyBTz** despite a larger energy difference between the monomer units of the former (Figure 4). These observations highlight the need to consider the fundamental principles of perturbation MO theory in selecting monomeric units using the A-A design strategy; namely, that the strength of the interaction is not only dependent on the relative orbital energies of the component moieties, but also a function of the degree of orbital overlap which affects the final shape of the product orbitals.<sup>54</sup> The differences in the spatial extent of positive and negative charge carriers has implications for charge transport<sup>55,56</sup> between holes and electrons in thin films,<sup>57</sup> which can affect the performance of these materials in OFET devices.<sup>58</sup>

# 2.4 Field Effect Electron Transport

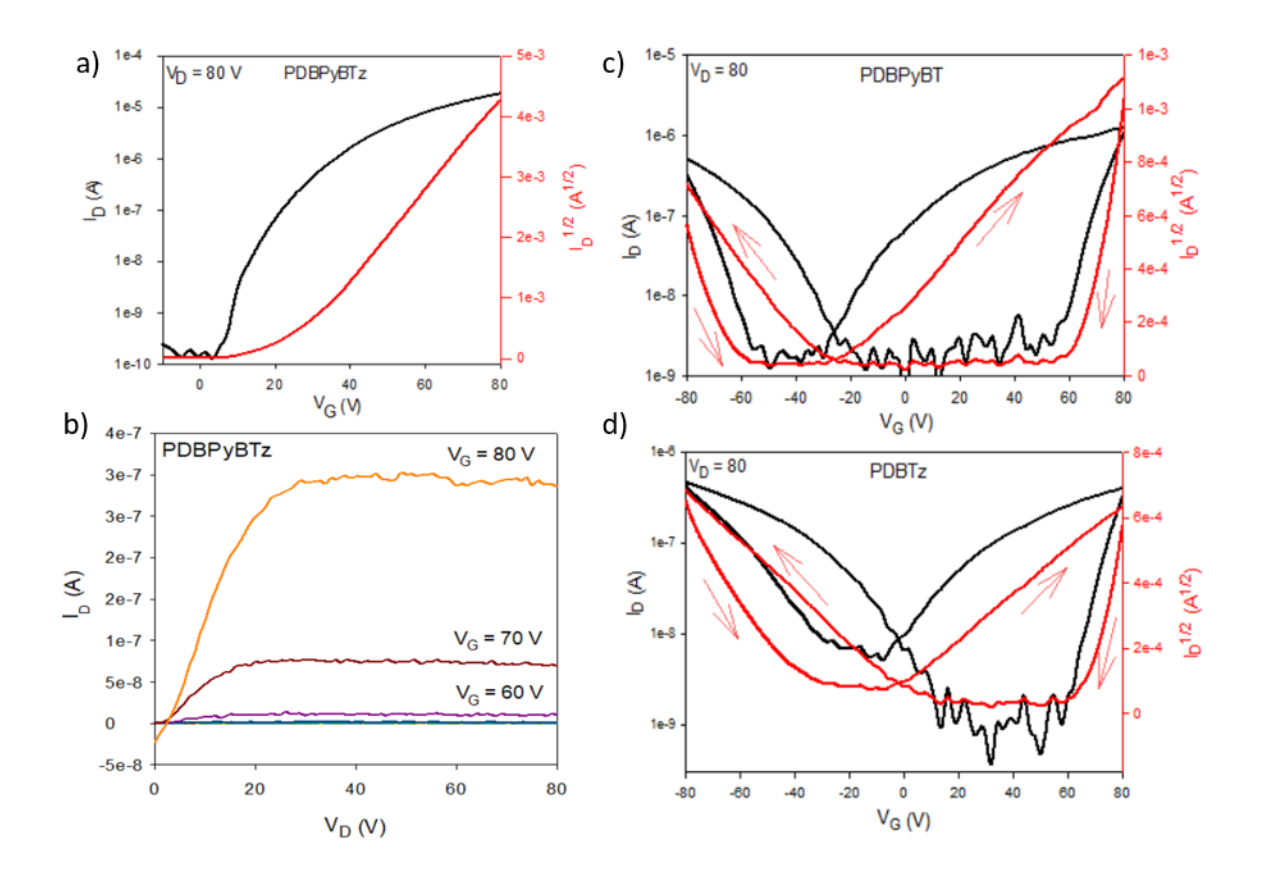


**Figure 5.** Transfer (a) and output (b) characteristics of PDBPyBTz, and transfer characteristics of PDBTz (c) and PDBPyBT (d) devices blade-coated from p-xylene.

Table 2. Electron transport properties of PDBPyBTz on OTS-modified BGBC OFET devices\*

Dolumor	Solvent	Annealing	$\mu_{e}$ (cm $^{2}$ V $^{-1}$	V (\( \)	1 //	
Polymer	Solveni	Armeaning	Average	Max	V <sub>Th</sub> (V)	I <sub>ON</sub> /I <sub>OFF</sub>
	CHCl₃	Pristine	0.010 ± 0.002	0.013	23.1 ± 2.2	10 <sup>4</sup> -10 <sup>5</sup>
		100 °C	$0.021 \pm 0.007$	0.054	$22.6 \pm 2.9$	10 <sup>2</sup> -10 <sup>4</sup>
		125 °C	0.017 ± 0.001	0.019	18.0 ± 1.3	10 <sup>2</sup> -10 <sup>6</sup>
DDDD: DT-		150 °C	0.017 ± 0.001	0.019	20.1 ± 3.4	10 <sup>3</sup> -10 <sup>4</sup>
PDBPy-BTz	p-xylene	Pristine	$0.018 \pm 0.007$	0.023	27.5 ± 1.0	10 <sup>4</sup> -10 <sup>5</sup>
		100 °C	0.021 ± 0.002	0.027	26.2 ± 1.5	10 <sup>2</sup> -10 <sup>5</sup>
		125 °C	$0.020 \pm 0.001$	0.023	$23.9 \pm 2.5$	10 <sup>4</sup> -10 <sup>5</sup>
		150 °C	$0.023 \pm 0.002$	0.030	$30.5 \pm 3.5$	10 <sup>3</sup> -10 <sup>5</sup>

\* OFET characterization results based on 6 devices for each condition. Annealing performed over 30 minute intervals. Data for each condition was taken over six devices.

The charge carrier properties of PDBPyBTz were evaluated in bottom-gate, bottom-contact (BGBC) organic field effect transistor (OFET) devices using a p-doped Si substrate as the gate electrode, with a 300 nm thick layer of thermally grown SiO<sub>2</sub> as the gate dielectric (full details of device fabrication and structure given in the supporting information). Au source and drain contacts (50 nm of Au with 3 nm of Cr as the adhesion layer) with fixed channel dimensions (50 µm in length and 2 mm in width) were deposited via E-beam using a photolithography lift-off process. After depositing the contacts, the SiO<sub>2</sub> surface was modified with OTS-18 to minimize surface charge trapping. The analogous polymers PDBTz and PDBPyBT were also incorporated into OFET devices for comparison. Similar to a previous report of an all-acceptor DPP-polymer, 18 PDBPyBTz-based OFETs demonstrated solely n-channel transport with no obvious source-drain current under negative gate voltage even when Au electrodes were used (Figure 5 and Figure S19). The average electron mobility (μ<sub>e</sub>) of blade-coated **PDBPyBTz** devices were approximately 0.02 cm<sup>2</sup>V<sup>-1</sup>s<sup>-1</sup>, with a maximum  $\mu_e$  of 0.054 cm<sup>2</sup>V<sup>-1</sup>s<sup>-1</sup> (**Table 2**, plot of mobility vs. gate bias shown in Figure S20). There were only negligible differences in n-channel performance between spin- and blade-coated devices of PDBPyBTz (Table S2). In contrast, the analogous PDBPyBT and PDBTz copolymers exhibited ambipolar transport in devices fabricated under the same conditions (Figure 5). PDBPyBT blade-coated from p-xylene had an average μ<sub>e</sub> of 4.4x10<sup>-4</sup> cm<sup>2</sup>V<sup>-1</sup>s<sup>-1</sup>, while PDBTz deposited under the same conditions had an average  $\mu_e$  of  $2.2x10^{-4}\,\text{cm}^2\text{V}^{-1}\text{s}^{-1}$ ; both these values are two orders of magnitude below that seen for PDBPyBTz. The hysteresis patterns and positive shift of V<sub>T</sub> with each consecutive sweep on a single channel of both PDBPyBT and PDBTz can be attributed to the presence of electron traps that are injected as the device is placed under positive gate bias (Figure S21).<sup>59</sup> This causes discrepancies in V<sub>T</sub> across the channel that invalidate the assumptions of the Schockley equation, which precludes reliable hole mobility extraction.<sup>8,60</sup> It is interesting that the polymer with the

highest estimated frontier energy levels (and hence the least efficient electron injection with Au contacts) (**Figure 4**) was the only polymer that demonstrated solely n-channel transport. As all the devices in this study were fabricated simultaneously under the same conditions, we speculate that hole-traps specific to **PDBPyBTz** are the source of the unipolar charge transport. Bithiazole has been reported to form complexes with Lewis acids<sup>61</sup> and we speculate that such interactions may be occurring with the BTz moieties in **PDBPyBTz** and the hole charge carriers, effectively blocking hole transport.

# 2.5 Thin Film Morphology and Microstructure

The surface morphologies of **PDBPyBTz**, **PDBTz**, and **PDBPyBT** films blade-coated onto OTS-modified Si-substrates were characterized using tapping-mode atomic force microscopy (AFM) (Figures S22 and S23, SI). Non-annealed films blade-coated from both p-xylene and CHCl<sub>3</sub> solutions of **PDBPyBTz** exhibited similar morphologies, as can be seen in Figure S22. The similarity in the surface morphologies is consistent with the similarity in OFET device performance parameters observed between films cast from the two solvents, as film morphology is known to have a profound influence on charge transport properties. 62–64 Upon annealing at 150 °C for 30 minutes, the film coated from p-xylene solution developed a network formation on the surface, while that coated from CHCl<sub>3</sub> had no discernable morphology (Figure S21). AFM images of pristine PDBPyBT and PDBTz devices blade-coated from p-xylene can be seen in Figure S23.

To investigate **PDBPyBTz** chain packing, we carried out two-dimensional grazing-incidence wide-angle X-ray scattering (2D-GIWAXS) on blade-coated films cast from p-xylene onto OTS-modified Si substrates (300 nm SiO<sub>2</sub> dielectric on heavily p-doped Si) (Figure 7; x-ray scattering patterns shown in Figure S24). An isotropic ring can be observed at  $2\theta = \sim 25^{\circ}$  corresponding to a d-spacing of 0.417 nm (4.17 Å), which is on the order typical of  $\pi$ - $\pi$  stacking distances. The scattering intensities of this ring are similar in magnitude in both the [h00] and [0k0] directions. The well-defined diffraction peak at  $2\theta = \sim 6^{\circ}$  corresponding to a d-spacing of 2.11 nm (21.1 Å) is attributed to highly ordered lamellar d-spacing between the polymer chains and is of higher intensity in the <h00> direction than the <0k0> direction.

The <200> peak at  $2\theta = \sim 11^{\circ}$  indicates a higher order of lamellar spacing between the 2-octyldodecyl side-chains separating the polymer chains. Herman's orientation parameter (S, calculation details provided in SI) was calculated to quantify the orientation distribution of the first-order lamellar stacking peak ([100]) and resulted in an S value of 0.46, indicating a mainly edge-on orientation. Such an edge-on orientation is conducive to in-plane charge-transport mobilities, such as those measured in OFET devices.

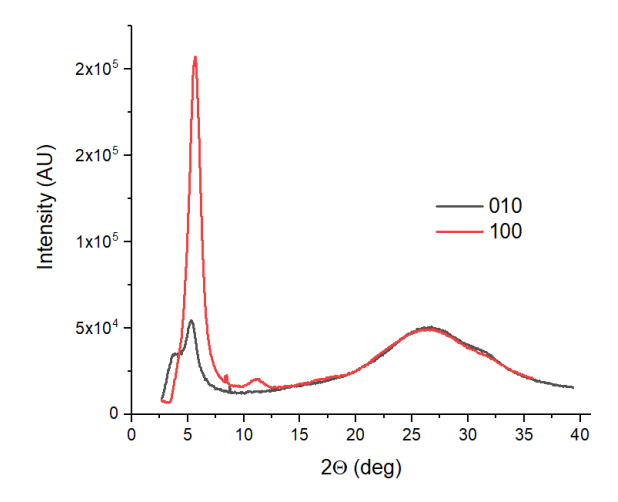


Figure 7. GIWAXS lineaut patterns of blade-coated PDBPyBTz thin films on OTS-modified Si/SiO2 surfaces.

# 3.0 Conclusion

A semiconducting polymer, PDBPyBTz, was designed using the all-acceptor design strategy and prepared by Stille copolymerization of the electron deficient 2,2'-bithiazole and bispyridinyl diketopyrrolopyrrole moieties. PDBPyBTz has a high electron affinity of 3.87 eV, suggesting good ambient stability. Spectral properties include a low optical bandgap of 1.47 eV and a  $\lambda_{max}$  of 656 nm for the material in thin-film form. BGBC OFET devices fabricated using blade-coated PDBPyBTz active layers demonstrated unipolar n-channel charge transport, with electron mobilities reaching 0.02 cm<sup>2</sup>V<sup>-1</sup>s<sup>-1</sup>. That the IP and EA values of PDBPyBTz were lower (which corresponds to frontier levels higher in energy) in comparison with the analogous PDBPyBT and PDBTz copolymers comprised of more electron-rich monomers was a surprising result, which highlights the need to consider orbital parity and wavefunction distribution

between component units in polymeric semiconductors in determining structure-property relationships of

product materials and electronic compatibility between candidate monomer pairs. We believe the

semiconducting performance and optoelectronic properties of PDBPyBTz make it a versatile material for

further studies in organic electronics with opportunities for optimizing its charge transport performance in

device applications. In addition to its demonstrated potential in transistor devices, PDBPyBTz is also a

particularly promising candidate for incorporation into organic photovoltaics as an acceptor material. This

study demonstrates the successful implementation of the all-acceptor design strategy in developing an

electron-deficient conjugated polymer amenable to unipolar n-channel transport in OFET devices. Further,

preliminary device performance results highlight the complex relationships between molecular structure,

photophysical characteristics and solution process protocols associated with the implementation of

conjugated polymers into optoelectronic devices.

ASSOCIATED CONTENT

Supporting Information. Synthetic schemes, experimental details, spectral data, thermal analysis, calculation details, electrochemical scans, and device fabrication procedures provided in the Supporting Information. This material is available free

of charge at http://pubs.acs.org.

**AUTHOR INFORMATION** 

**Corresponding Author** 

E-mail: ereichmanis@chbe.gatech.edu

**Current Address** 

\*Applied Materials, Inc. 3050 Bowers Avenue, Santa Clara, CA 95054-3299 United States

4.0 Acknowledgement

Support from the National Science Foundation, DMR-1809495 is gratefully acknowledged. CB and MM also appreciate support from the NSF NESAC IGERT (DGE 1069138). ER appreciates support

associated with funds associated with the Pete Silas Chair in Chemical Engineering. JLB acknowledges support from the Office of Naval Research under Award No. N00014-17-1-2208. This work was performed in part at the Georgia Tech Institute for Electronics and Nanotechnology, a member of the

National Nanotechnology Coordinated Infrastructure, which is supported by the National Science Foundation (Grant ECCS-1542174). The authors would also like to thank Dr. John Reynolds, Dr. Bing Xu, Ian Pelse, Bronson Cox, Brian Khau, Dr. Carlos Silva and Dr. Ilaria Bargigia of the School of

Chemistry and Biochemistry and the Georgia Tech Polymer Network at the Georgia Institute of Technology for valuable discussions, high-temp GPC characterization, GIWAXS spectra, and

fluorescence spectra.

18

# 5.0 References

- (1) Gelinck, G.; Heremans, P.; Nomoto, K.; Anthopoulos, T. D. Organic Transistors in Optical Displays and Microelectronic Applications. *Adv. Mater.* **2010**, *22* (34), 3778–3798.
- (2) Arias, A. C.; MacKenzie, J. D.; McCulloch, I.; Rivnay, J.; Salleo, A. Materials and Applications for Large Area Electronics: Solution-Based Approaches. *Chem. Rev.* **2010**, *110* (1), 3–24.
- (3) Torsi, L.; Magliulo, M.; Manoli, K.; Palazzo, G. Organic Field-Effect Transistor Sensors: A Tutorial Review. *Chem. Soc. Rev.* **2013**, *42* (22), 8612.
- (4) Sirringhaus, H. 25th Anniversary Article: Organic Field-Effect Transistors: The Path Beyond Amorphous Silicon. *Adv. Mater.* **2014**, *26*, 1319–1335.
- (5) Wang, C.; Dong, H.; Hu, W.; Liu, Y.; Zhu, D. Semiconducting π-Conjugated Systems in Field-Effect Transistors: A Material Odyssey of Organic Electronics. *Chem. Rev.* **2012**, *112*, 2208–2267.
- (6) Fei, Z.; Han, Y.; Gann, E.; Hodsden, T.; Chesman, A. S. R.; McNeill, C. R.; Anthopoulos, T. D.; Heeney, M. Alkylated Selenophene-Based Ladder-Type Monomers via a Facile Route for High-Performance Thin-Film Transistor Applications. *J. Am. Chem. Soc.* **2017**, *139* (25), 8552–8561.
- (7) Tseng, H. R.; Phan, H.; Luo, C.; Wang, M.; Perez, L. A.; Patel, S. N.; Ying, L.; Kramer, E. J.; Nguyen, T. Q.; Bazan, G. C.; et al. High-Mobility Field-Effect Transistors Fabricated with Macroscopic Aligned Semiconducting Polymers. *Adv. Mater.* **2014**, *26* (19), 2993–2998.
- (8) Quinn, J. T. E.; Zhu, J.; Li, X.; Wang, J.; Li, Y. Recent Progress in the Development of N-Type Organic Semiconductors for Organic Field Effect Transistors. *J. Mater. Chem. C* **2017**, *5* (34), 8654–8681.
- (9) Zhao, X.; Zhan, X. Electron Transporting Semiconducting Polymers in Organic Electronics. *Chem. Soc. Rev.* **2011**, *40* (7), 3728.
- (10) Wang, Y.; Hasegawa, T.; Matsumoto, H.; Michinobu, T. Significant Improvement of Unipolar N-Type Transistor Performances by Manipulating the Coplanar Backbone Conformation of Electron-Deficient Polymers via Hydrogen-Bonding. *J. Am. Chem. Soc.* **2019**.
- (11) Cornil, J.; Brédas, J. L.; Zaumseil, J.; Sirringhaus, H. Ambipolar Transport in Organic Conjugated Materials. *Adv. Mater.* **2007**, *19* (14), 1791–1799.
- (12) Ortiz, R. P.; Herrera, H.; Seoane, C.; Segura, J. L.; Facchetti, A.; Marks, T. J. Rational Design of Ambipolar Organic Semiconductors: Is Core Planarity Central to Ambipolarity in Thiophene-Naphthalene Semiconductors? *Chem. A Eur. J.* **2012**, *18* (2), 532–543.
- (13) Zaumseil, J.; Sirringhaus, H. Electron and Ambipolar Transport in Organic Field-Effect Transistors. *Chem. Rev.* **2007**, *107*, 1296–1323.
- (14) Kim, F. S.; Guo, X.; Watson, M. D.; Jenekhe, S. A. High-Mobility Ambipolar Transistors and High-Cain Inverters from a Donor-Acceptor Copolymer Semiconductor. *Adv. Mater.* **2010**, *22* (4), 478–482.
- (15) Jung, I. H.; Lo, W. Y.; Jang, J.; Chen, W.; Zhao, D.; Landry, E. S.; Lu, L.; Talapin, D. V.; Yu, L. Synthesis and Search for Design Principles of New Electron Accepting Polymers for All-Polymer Solar Cells. *Chem. Mater.* **2014**, *26* (11), 3450–3459.

- (16) Durban, M. M.; Kazarinoff, P. D.; Luscombe, C. K. Synthesis and Characterization of Thiophene-Containing Naphthalene Diimide n-Type Copolymers for OFET Applications. *Macromolecules* **2010**, *43* (15), 6348–6352.
- (17) Guo, X.; Ortiz, R. P.; Zheng, Y.; Hu, Y.; Noh, Y. Y.; Baeg, K. J.; Facchetti, A.; Marks, T. J. Bithiophene-Imide-Based Polymeric Semiconductors for Field-Effect Transistors: Synthesis, Structure-Property Correlations, Charge Carrier Polarity, and Device Stability. *J. Am. Chem. Soc.* **2011**, *133* (5), 1405–1418.
- (18) Yuan, Z.; Fu, B.; Thomas, S.; Zhang, S.; Deluca, G.; Chang, R.; Lopez, L.; Fares, C.; Zhang, G.; Bredas, J.; et al. Unipolar Electron Transport Polymers: A Thiazole Based All-Electron Acceptor Approach. *Chem. Mater.* **2016**, *28*, 6045–6049.
- (19) Kim, G.; Han, A.-R.; Lee, H. R.; Lee, J.; Oh, J. H.; Yang, C. Acceptor–acceptor Type Isoindigo-Based Copolymers for High-Performance n-Channel Field-Effect Transistors. *Chem. Commun.* 2014, 50 (17), 2180.
- (20) Lee, J. K.; Gwinner, M. C.; Berger, R.; Newby, C.; Zentel, R.; Friend, R. H.; Sirringhaus, H.; Ober, C. K. High-Performance Electron-Transporting Polymers Derived from a Heteroaryl Bis(Trifluoroborate). J. Am. Chem. Soc. 2011, 133 (26), 9949–9951.
- (21) Stalder, R.; Mei, J.; Subbiah, J.; Grand, C.; Estrada, L. A.; So, F.; Reynolds, J. R. N-Type Conjugated Polyisoindigos. *Macromolecules* **2011**, *44* (16), 6303–6310.
- (22) Zhao, X.; Wen, Y.; Ren, L.; Ma, L.; Liu, Y.; Zhan, X. An Acceptor-Acceptor Conjugated Copolymer Based on Perylene Diimide for High Mobility n-Channel Transistor in Air. *J. Polym. Sci. Part A Polym. Chem.* **2012**, *50* (20), 4266–4271.
- (23) Wang, Y.; Guo, H.; Harbuzaru, A.; Uddin, M. A.; Ling, S.; Yu, J.; Tang, Y.; Sun, H.; Wang, Y.; Guo, H.; et al. (Semi)Ladder-Type Bithiophene Imide-Based All-Acceptor Semiconductors: Synthesis, Structure-Property Correlations, and Unipolar n-Type Transistor Performance. *J. Am. Chem. Soc.* **2018**, *140*, 6096–6108.
- (24) Xiao, M.; Onwubiko, A.; Yue, W.; Sirringhaus, H.; Wadsworth, A.; Nikolka, M.; Baran, D.; Chen, H.-Y.; McCulloch, I.; White, A. J. P. A Thieno[2,3-b]Pyridine-Flanked Diketopyrrolopyrrole Polymer as an n-Type Polymer Semiconductor for All-Polymer Solar Cells and Organic Field-Effect Transistors. *Macromolecules* **2017**, *51* (1), 71–79.
- (25) Letizia, J. A.; Salata, M. R.; Tribout, C. M.; Facchetti, A.; Ratner, M. A.; Marks, T. J. N-Channel Polymers by Design: Optimizing the Interplay of Solubilizing Substituents, Crystal Packing, and Field-Effect Transistor Characteristics in Polymeric Bithiophene-Imide Semiconductors. *J. Am. Chem. Soc.* **2008**, *130* (30), 9679–9694.
- (26) Yan, H.; Chen, Z.; Zheng, Y.; Newman, C.; Quinn, J. R.; Dötz, F.; Kastler, M.; Facchetti, A. A High-Mobility Electron-Transporting Polymer for Printed Transistors. *Nature* **2009**, *457* (7230), 679–686.
- (27) Sun, B.; Hong, W.; Yan, Z.; Aziz, H.; Li, Y. Record High Electron Mobility of 6.3 Cm2V-1s-1 Achieved for Polymer Semiconductors Using a New Building Block. *Adv. Mater.* **2014**, *26* (17), 2636–2642.
- (28) Li, Y.; Sonar, P.; Singh, S. P.; Soh, M. S.; Van Meurs, M.; Tan, J. Annealing-Free High-Mobility Diketopyrrole-Quaterthiophene Copolymer for Solution-Processed Organic Thin Film Transistors. *J. Am. Chem. Soc.* **2011**, *133* (7), 2198–2204.
- (29) Sun, B.; Hong, W.; Aziz, H.; Li, Y. A Pyridine-Flanked Diketopyrrolopyrrole (DPP)-Based

- Donor–acceptor Polymer Showing High Mobility in Ambipolar and n-Channel Organic Thin Film Transistors. *Polym. Chem.* **2015**, *6* (6), 938–945.
- (30) Mueller, C. J.; Singh, C. R.; Fried, M.; Huettner, S.; Thelakkat, M. High Bulk Electron Mobility Diketopyrrolopyrrole Copolymers with Perfluorothiophene. *Adv. Funct. Mater.* **2015**, *25* (18), 2725–2736.
- (31) Nielsen, C. B.; Turbiez, M.; Mcculloch, I. Recent Advances in the Development of Semiconducting DPP-Containing Polymers for Transistor Applications. *Adv. Mater.* **2013**, *25*, 1859–1880.
- (32) Su, H. L.; Sredojevic, D. N.; Bronstein, H.; Marks, T. J.; Schroeder, B. C.; Al-Hashimi, M. Bithiazole: An Intriguing Electron-Deficient Building for Plastic Electronic Applications. *Macromol. Rapid Commun.* **2017**, *38*, 1600610.
- (33) Bronstein, H.; Hurhangee, M.; Fregoso, E. C.; Beatrup, D.; Soon, Y. W.; Huang, Z.; Hadipour, A.; Tuladhar, P. S.; Rossbauer, S.; Sohn, E. H.; et al. Isostructural, Deeper Highest Occupied Molecular Orbital Analogues of Poly(3-Hexylthiophene) for High-Open Circuit Voltage Organic Solar Cells. *Chem. Mater.* **2013**, *25* (21), 4239–4249.
- (34) Fu, B.; Wang, C. Y.; Rose, B. D.; Jiang, Y.; Chang, M.; Chu, P. H.; Yuan, Z.; Fuentes-Hernandez, C.; Kippelen, B.; Bredas, J.-L.; et al. Molecular Engineering of Nonhalogenated Solution-Processable Bithiazole-Based Electron-Transport Polymeric Semiconductors. *Chem. Mater.* **2015**, 27 (8), 2928–2937.
- (35) Hassan, J.; Lavenot, L.; Gozzi, C.; Lemaire, M. A Convenient Catalytic Route to Symmetrical Functionalized Bithiophenes. *Tetrahedron Lett.* **1999**, *40* (5), 857–858.
- (36) Guo, F.; Liu, X.; Ding, Y.; Kong, F.; Chen, W.; Zhou, L.; Dai, S. Broad Spectral-Response Organic D–A–π–A Sensitizer with Pyridine-Diketopyrrolopyrrole Unit for Dye-Sensitized Solar Cells. *RSC Adv.* **2016**, *6* (16), 13433–13441.
- (37) Frisch, M. J.; Trucks, G. W.; Schlegel, H. B.; Scuseria, G. E.; Robb, A.; Cheeseman, J. R.; Scalmani, G.; Barone, V.; Petersson, G. A.; Nakatsuji, H.; et al. Gaussian 09, Revision A.01. Gaussian, Inc.: Wallingford, CT 2016.
- (38) Stein, T.; Kronik, L.; Baer, R. Reliable Prediction of Charge Transfer Excitations in Molecular Complexes Using Time-Dependent Density Functional Theory. *J. Am. Chem. Soc* **2009**, *131*, 2818–2820.
- (39) Korzdorfer, T.; Bredas, J.-L. Organic Electronic Materials: Recent Advances in the DFT Description of the Ground and Excited States Using Tuned Range-Separated Hybrid Functionals. *Acc. Chem. Res.* **2014**, *47*, 3284–3291.
- (40) Reichardt, C. Solvatochromic Dyes as Solvent Polarity Indicators. *Chem. Rev.* **1994**, *94* (8), 2319–2358.
- (41) Spano, F. C. The Spectral Signatures of Frenkel Polarons in H-and J-Aggregates. *Acc. Chem. Res.* **2009**, *43* (3), 429–439.
- (42) Kasha, M. Energy Transfer Mechanisms and the Molecular Exciton Model for Molecular Aggregates. *Radiat. Res.* **1963**, *20* (1), 55–70.
- (43) Spano, F. C.; Silva, C. H- and J-Aggregate Behavior in Polymeric Semiconductors. *Annu. Rev. Phys. Chem.* **2014**, *65*, 477–500.

- (44) Schwartz, B. J. Conjugated Polymers as Molecular Materials: How Chain Conformation and Film Morphology Influence Energy Transfer and Interchain Interactions. *Annu. Rev. Phys. Chem.* **2003**, 54 (1), 141–172.
- (45) Hansen, W. N.; Hansen, G. J. Absolute Half-Cell Potential: A Simple Direct Measurement. *Phys. Rev. A* **1987**, *36* (3), 1396–1402.
- (46) Pavlishchuk, V. V.; Addison, A. W. Conversion Constants for Redox Potentials Measured versus Different Reference Electrodes in Acetonitrile Solutions at 25°C. *Inorganica Chim. Acta* **2000**, 298 (1), 97–102.
- (47) Cardona, C. M.; Li, W.; Kaifer, A. E.; Stockdale, D.; Bazan, G. C. Electrochemical Considerations for Determining Absolute Frontier Orbital Energy Levels of Conjugated Polymers for Solar Cell Applications. *Adv. Mater.* **2011**, *23*, 2367–2371.
- (48) Bredas, J.-L. Mind the Gap! *Mater. Horizons* **2014**, *1*, 17–19.
- (49) de Leeuw, D. M.; Simenon, M. M. J.; Brown, a. R.; Einerhand, R. E. F. Stability of N-Type Doped Conducting Polymers and Consequences for Polymeric Microelectronic Devices. *Synth. Met.* **1997**, *87*, 53–59.
- (50) Yuan, Z.; Buckley, C.; Thomas, S.; Zhang, G.; Bargigia, I.; Wang, G.; Fu, B.; Silva, C.; Brédas, J.; Reichmanis, E. A Thiazole–Naphthalene Diimide Based N-Channel Donor–Acceptor Conjugated Polymer. *Macromolecules* **2018**, *51*, 7320–7328.
- (51) Johansson, T.; Mammo, W.; Svensson, M.; Andersson, R.; Ingana, O. Electrochemical Bandgaps of Substituted Polythiophenes. *J. Mater. Chem.* **2003**, *13*, 1316–1323.
- (52) Bujak, P.; Kulszewicz-bajer, I.; Zagorska, M.; Maurel, V.; Wielgus, I.; Pron, A. Polymers for Electronics and Spintronics. *Chem. Soc. Rev.* **2013**, *42*, 8895–8999.
- (53) Brédas, J. L.; Silbey, R.; Boudreaux, D. S.; Chance, R. R. Chain-Length Dependence of Electronic and Electrochemical Properties of Conjugated Systems: Polyacetylene, Polyphenylene, Polythiophene, and Polypyrrole. *J. Am. Chem. Soc.* **1983**, *105* (22), 6555–6559.
- (54) Carey, F. A.; Sundberg, R. J. *Advanced Organic Chemistry Part A: Structure and Mechanisms*, 5th ed.; Springer: New York, 2007.
- (55) Marcus, R. A. Electron Transfer Reactions. Rev. Mod. Phys. **1993**, 65 (3), 599–610.
- (56) Barbara, P. F.; Meyer, T. J.; Ratner, M. A. Contemporary Issues in Electron Transfer Research. *J. Phys. Chem.* **1996**, *3654* (96), 13148–13168.
- (57) Olivier, Y.; Lemaur, V.; Brédas, J. L.; Cornil, J. Charge Hopping in Organic Semiconductors: Influence of Molecular Parameters on Macroscopic Mobilities in Model One-Dimensional Stacks. *J. Phys. Chem. A* **2006**, *110* (19), 6356–6364.
- (58) Hulea, I. N.; Fratini, S.; Xie, H.; Mulder, C. L.; Iossad, N. N.; Rastelli, G.; Ciuchi, S.; Morpurgo, A. F. Tunable Frohlich Polarons in Organic Single-Crystal Transistors. *Nat. Mater.* **2006**, *5*, 982–986.
- (59) Okachi, T.; Kashiki, T.; Ohya, K. Device Operation Mechanism of Field-Effect Transistors with High Mobility Donor-Acceptor Polymer Semiconductors. *Proc. SPIE* **2015**, *14* (4), 420–426.
- (60) Horowitz, G.; Hajlaoui, R.; Bouchriha, H.; Bourguiga, R.; Hajlaoui, M. Concept of 'threshold Voltage' in Organic Field-Effect Transistors. *Adv. Mater.* **1998**, *10* (12), 923–927.

- (61) Findlater, M.; Swisher, N. S.; White, P. S. Synthesis and Structure of Boron-Bithiazole Complexes. *Eur. J. Inorg. Chem.* **2010**, *302* (34), 5379–5382.
- (62) Virkar, A. A.; Mannsfeld, S.; Bao, Z.; Stingelin, N. Organic Semiconductor Growth and Morphology Considerations for Organic Thin-Film Transistors. *Adv. Mater.* **2010**, *22* (34), 3857–3875.
- (63) Botiz, I.; Stingelin, N. Influence of Molecular Conformations and Microstructure on the Optoelectronic Properties of Conjugated Polymers. *Materials*. **2014**, *7* (3), 2273–2300.
- (64) Rivnay, J.; Mannsfeld, S. C. B.; Miller, C. E.; Salleo, A.; Toney, M. F. Quantitative Determination of Organic Semiconductor Microstructure from the Molecular to Device Scale. *Chem. Rev.* **2012**, *112* (10), 5488–5519.
- (65) Perez, L. A.; Zalar, P.; Ying, L.; Schmidt, K.; Toney, M. F.; Nguyen, T. Q.; Bazan, G. C.; Kramer, E. J. Effect of Backbone Regioregularity on the Structure and Orientation of a Donor-Acceptor Semiconducting Copolymer. *Macromolecules* 2014, 47 (4), 1403–1410.

# 6.0 Table of contents/Abstract Graphic

